

## Search for Collective Effects in Very High Spin States of $^{152}\text{Dy}$

Y. Schutz, J. P. Vivien, F. A. Beck, T. Byrski, C. Gehringer, and J. C. Merdinger  
*Centre de Recherches Nucléaires et Université Louis Pasteur, F-67037 Strasbourg Cédex, France*

and

J. Dudek, W. Nazarewicz,<sup>(a)</sup> and Z. Szymanski  
*Institute of Theoretical Physics, Warsaw University, PL-00-681 Warsaw, Poland*  
 (Received 14 January 1982)

Theoretical calculations based on the rotating Woods-Saxon potential with optimized parameters indicate appearance of the superdeformed shapes with  $\beta_2=0.6$  already at  $I \approx 52$  and simultaneously the triaxial-configuration minimum ( $\gamma \approx 30^\circ$ ) with  $\beta_2 \approx 0.3$ . Two values of the moments of inertia viz.  $2\mathcal{G}^{(2)} \approx (167 \text{ and } 125)\hbar^2 \text{ MeV}^{-1}$  were deduced from our  $E_\gamma$ - $E_\gamma$  correlation measurement.

PACS numbers: 21.10.Re, 21.10.Ft, 27.70.+q

In the last few years single-particle effects in high-spin excitations have been extensively studied in several rare-earth neutron-deficient nuclei with  $Z$  close to  $Z_0=64$ . Nuclei revealing such effects are distinguished by their irregular  $E$  vs  $I$  dependence of the yrast line. Spins of these nuclei are predominantly composed of contributions from a few nucleons which align their angular momenta with the nuclear symmetry axis. Such nuclei are expected to be spherical or slightly oblate ( $\beta_2 \approx 0.1$ ,  $\gamma = 60^\circ$ ) at least within some range of spin.

One of the best studied in this group is the  $^{152}\text{Dy}$  nucleus in which the yrast line was established up to  $I=38\hbar$ .<sup>1</sup> However, up to now there are only a few facts known experimentally about the properties of this nucleus for very high ( $I > 38\hbar$ ) spins. In the unresolved part of the spectrum of this nucleus, for  $E_\gamma > 1 \text{ MeV}$ , a presence of characteristic bump in the intensity-vs- $E_\gamma$  plot has been reported<sup>2</sup> and shown to consist<sup>3</sup> essentially of stretched  $E2$  transitions.

The aim of this paper is to investigate the structure of  $^{152}\text{Dy}$  at very high ( $I \geq 40\hbar$ ) angular momenta. This has been done both theoretically, by calculating the total energy surfaces as functions of spin and deformation, and experimentally, by analyzing the unresolved (quasicontinuum) part of the spectrum with the help of the  $E_\gamma$ - $E_\gamma$  correlation technique.

In our calculations the shell correction method of Strutinsky has been used, generalized to the case of rotation as in Ref. 4. Here, however, we differ from the above paper by using the deformed Woods-Saxon potential with especially optimized parameters. With these parameters both the slope of the yrast line and the spin-parity assignments were described well for  $I$

$< 38\hbar$  states of  $^{152}\text{Dy}$  and for a few other nuclei from the vicinity of  $^{146}\text{Gd}$  (these calculations are presented elsewhere<sup>5</sup>). Our calculations differ also from the recent study<sup>6</sup> where the rotating potential of Nilsson was employed. In the studies of high-spin rotation the Woods-Saxon and Nilsson potentials reveal systematic differences which result from the presence of the  $\bar{I}^2$  term in the Nilsson potential. In particular it was demonstrated<sup>7</sup> that the presence of the  $\bar{I}^2$  term gives rise to an overestimate in the aligned single-particle angular momentum of about, roughly, 30%.

The results of the total energy calculations are displayed in Fig. 1 for  $I=(38, 46, 50, 52, 56, \text{ and } 60)\hbar$ . Calculations show that at  $I=38\hbar$  a pronounced minimum corresponding to an oblate ( $\gamma=60^\circ$ ) deformation exists according to what one should expect from the characteristic irregular deexcitation pattern for this nucleus at  $I < 40\hbar$ . For spins  $38 < (I/\hbar) < 46$  the energy landscape quickly becomes more complicated revealing a well pronounced valley for  $\gamma \approx 30^\circ$  with a minimum at  $\beta_2 \approx 0.28$ . Both the fact of the triaxial shape at the minimum and the relatively flat bottom of the valley for  $\gamma \approx 30^\circ$  suggest that the typical deexcitation pattern is a superposition of many transitions of comparable energies, at least for some spins above  $I=40\hbar$ . These transitions would correspond to the moments of inertia varying from about  $2\mathcal{G}^{(2)} \approx 120\hbar^2 \text{ MeV}^{-1}$  ( $\beta_2 \sim 0.15$ ) up to  $2\mathcal{G}^{(2)} \approx 140\hbar^2 \text{ MeV}^{-1}$  ( $\beta_2 \sim 0.3$ ) and would contribute to the unresolved part of the spectrum. At still higher angular momentum, say  $I \sim 52\hbar$ , a secondary minimum corresponding to  $\beta_2 \sim 0.6$  appears relatively low above the one at  $\gamma \approx 30^\circ$ . One can expect that in this region of spin both minima can be fed with not too drastically dif-

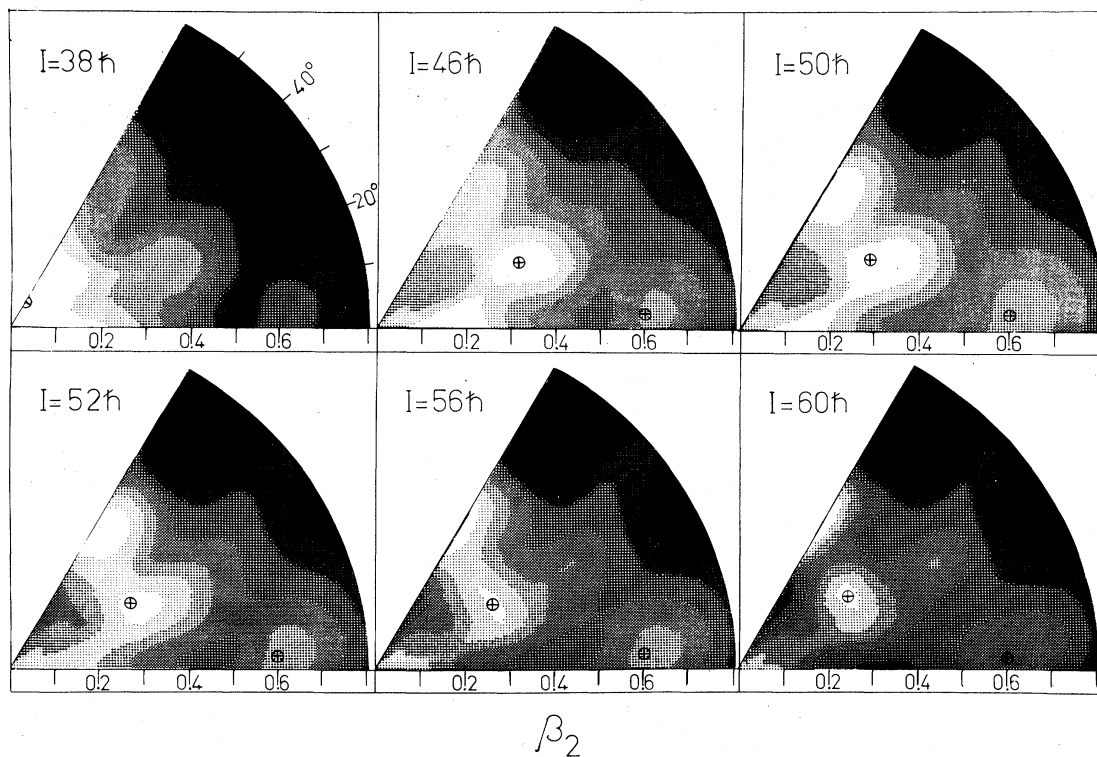


FIG. 1. Selected total-energy surfaces for  $^{152}\text{Dy}$ . The separation between the stripes is 2 MeV; crosses indicate the minima.

ferent intensities (see qualitative estimate, Fig. 2) and thus some transitions corresponding to the big moment of inertia ( $2g^{(2)} \sim 170\hbar^2 \text{ MeV}^{-1}$ ) can be expected (compare with Fig. 3). For still higher angular momentum (see  $I = 60\hbar$  part in Fig. 1) the secondary minimum grows higher above the one at  $\gamma \approx 30^\circ$  from where one may expect that feeding of the latter dominates. Finally, the "superdeformed" minimum at  $\beta_2 \approx 0.6$  becomes the absolute one but only for  $I > 88\hbar$ , in the calculations.

Another representation of the results in Fig. 1 is given in the diagram of  $E$  vs  $I$  and  $\beta_2(\gamma)$  in Fig. 2 from which one can see that the position of the superdeformed minimum relative to the one at  $\gamma \approx 30^\circ$  varies quite nonmonotonically with  $I$ .

To study experimentally the quasicontinuum  $\gamma$  rays, the  $E_\gamma - E_\gamma$  energy correlation technique proposed by Andersen *et al.*<sup>8</sup> has been applied. This kind of measurement extensively applied to rotational nuclei is especially well suited to study collective mechanisms and probe the band structure of a nucleus. The main problem one is faced with when using this technique is reduction of the background originating from not truly

correlated events. In the method usually proposed one calculates the deviation from the coin-

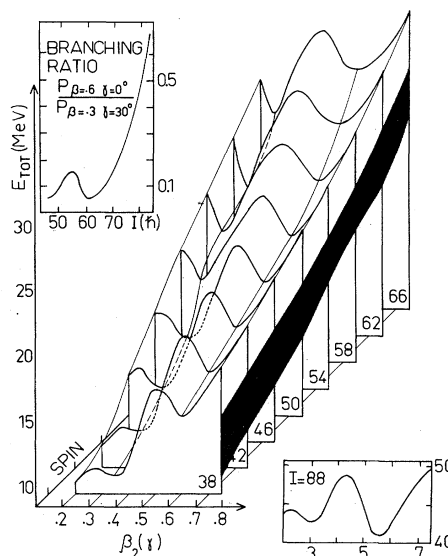


FIG. 2. Total energy of  $^{152}\text{Dy}$  along the minimum valley. Dark stripe illustrates the energy difference between the two minima. The upper inset illustrates an estimation of the relative feeding probability for the two collective minima.

idence rate. However, this method does not yield the absolute count value and may introduce spurious effects.<sup>9</sup> The procedure applied in this work unfolds the two-dimensional Ge(Li)  $\times$  Ge(Li) spectra starting from a careful study of the response function of each detector *in situ*. The resulting unfolded spectrum thus corresponds to a set of (photopeak)  $\times$  (photopeak) coincident events corresponding to energy-correlated transitions.

The experimental setup consists of an array of three Ge(Li) detectors fixed at  $0^\circ$ ,  $+90^\circ$ , and  $-90^\circ$ . The detectors were selected for their similar response functions and the energy gain was properly matched in order to be able to sum up the three possible pairs of  $\gamma$ - $\gamma$  events. The choice of Ge(Li) detectors was dictated by the energy resolution required to observe in the  $\gamma$ - $\gamma$  spectra a possible valleylike structure corresponding to a moment of inertia as high as  $200\hbar^2 \text{ MeV}^{-1}$ . In addition, the three Ge(Li) detectors were gated by a 12-in.  $\times$  12-in. NaI crystal covering a solid angle of nearly  $4\pi$  and used as a sum spectrometer. By subtraction of two energy-correlation spectra associated with high sum spectra, one obtains an  $E_\gamma$ - $E_\gamma$  spectrum in which the  $\gamma$  rays deexciting the highest excited states are enhanced<sup>10</sup> and the contribution of the neighboring nucleus  $^{151}\text{Dy}$  is totally eliminated. The  $^{152}\text{Dy}$  nucleus was produced in the reaction  $^{124}\text{Sn}(^{32}\text{S}, xn)$  induced by a sulfur beam with energy  $E_{\text{inc}} = 160 \text{ MeV}$  from the upgraded model MP tandem van de Graaf accelerator at Strasbourg. The 1-mg/cm<sup>2</sup> isotopically enriched tin target was evaporated on a 0.1-mm lead foil.

Figure 3 displays the difference of two unfolded  $\gamma$ - $\gamma$  spectra corresponding to two adjacent high-energy slices in the total energy spectrum. The two rows and columns observed through the diagonal are due in this compressed spectrum to the unresolved 525–541 and 967–991 keV transitions in  $^{152}\text{Dy}$  which cause additional coincidences all along these rows and columns. The most interesting features in this spectrum are two structures observed above 1 MeV where no discrete line contribution exists. Two valleys are observed: a narrow one (V1) which corresponds to transitions with energy  $1.1 \leq E_\gamma \leq 1.2 \text{ MeV}$  and a broad one (V2) with  $1.4 \leq E_\gamma \leq 1.6 \text{ MeV}$ . From the width of these valleys we deduced the corresponding moments of inertia which were found to be  $2\mathcal{J}^{(2)}/\hbar^2 = 167 \pm 20 \text{ MeV}^{-1}$  for V1 and  $2\mathcal{J}^{(2)}/\hbar^2 = 125 \pm 15 \text{ MeV}^{-1}$  for V2. The measured angular correlation ratio ( $0^\circ, 90^\circ$ ) to ( $90^\circ, 90^\circ$ ) indicates

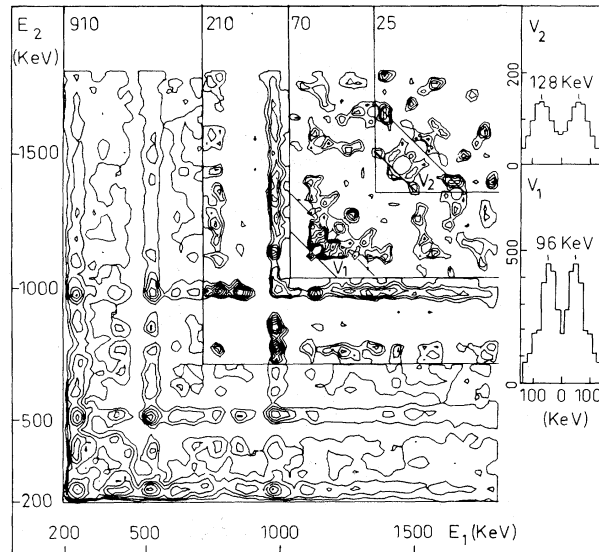


FIG. 3. Energy correlation spectrum for  $^{152}\text{Dy}$ . The maximum number of counts is indicated at the top of each sector. The insets represent cuts (as indicated in the contour plot) perpendicular to the diagonal.

that the ridges are due to coincidences between stretched quadrupole transitions.

In order to differentiate between the radiation which gives rise to the two valleys, an additional multiplicity measurement was performed. The experimental conditions were maintained the same as in the former experiment, except that two Ge(Li) detectors were replaced by two 5-in.  $\times$  6-in. NaI crystals set at  $\pm 90^\circ$ . Three types of events were registered from the Ge(Li) detectors set at  $0^\circ$  in coincidence with the NaI detectors: no NaI fired (fold 0), one NaI fired (fold 1), and two NaI fired (fold 2).<sup>11</sup> The mean multiplicity was deduced from the ratios fold 1 to fold 0 and fold 2 to fold 0. The value obtained from the transitions with energy  $1.1 \leq E_\gamma \leq 1.2 \text{ MeV}$  is  $\langle M \rangle = 29 \pm 3$ , and for  $1.4 \leq E_\gamma \leq 1.6 \text{ MeV}$ ,  $\langle M \rangle = 34 \pm 4$ . Despite the overlap of the two values within the error bars the systematics of the measured multiplicity versus energy indicates that the multiplicity for V2 is slightly larger than for V1.

From these values one can estimate the spin of the highest state fed in the rotational cascades. The cascade with a moment of inertia of  $167 \text{ MeV}^{-1}$  was found to start at  $I \approx (50 \pm 6)\hbar$  and the one with a moment of inertia of  $125 \text{ MeV}^{-1}$  at  $I \approx (60 \pm 8)\hbar$ . These results are in good agreement with the spin evaluation at the beginning of the yrast cascade  $I = 62\hbar$ , deduced from the calculated Baas<sup>12</sup> value for critical angular momentum.

It has been considered that during the cooling down of the compound nucleus each neutron takes away  $1.5\hbar$  and that on the average four statistical  $\gamma$  rays are emitted taking away  $0.5\hbar$  each.<sup>3</sup>

When comparing the results of the calculations with those deduced from the experiment, one is tempted to associate the first valley (V1) in Fig. 3 with the rotation of the superdeformed nucleus ( $\beta_2 \approx 0.6$ ,  $\gamma \approx 0^\circ$ ) with a rigid-body moment of inertia  $2g(\beta_2 \approx 0.6) = 165\hbar^2 \text{ MeV}^{-1}$  compared to the deduced value  $2g^{(2)} \approx 167\hbar^2 \text{ MeV}^{-1}$ . On the basis of our theoretical estimates we expect that at  $I > 60\hbar$ , but still less than  $\sim(80-88)\hbar$ , the secondary minimum lies rather high above the first one and thus we may expect a significant decrease in feeding the superdeformed configuration. Such an interpretation agrees with the above multiplicity estimates associated with the two valleys.

In summary:

(i) Our theoretical calculations based on the optimized Woods-Saxon potential reproduced the low-spin part of the yrast spectra of  $^{152}\text{Dy}$  and a few neighbors of  $^{146}\text{Gd}$ . With the same parameters of the Woods-Saxon potential the total energy surfaces have been calculated for very high spin states of  $^{152}\text{Dy}$  with the results of one oblate, one triaxial ( $\beta_2 \approx 0.3$ ,  $\gamma \approx 30^\circ$ ), and one superdeformed ( $\beta_2 \approx 0.6$ ,  $\gamma = 0^\circ$ ) minima competing with each other depending on the actual spin value.

(ii) The  $E_\gamma$ - $E_\gamma$  correlation technique results in the two valleys in the plot (Fig. 3) corresponding to  $2g^{(2)} \approx 125\hbar^2 \text{ MeV}^{-1}$  and  $2g^{(2)} \approx 167\hbar^2 \text{ MeV}^{-1}$ , respectively. The first value fits reasonably to the calculated  $2g^{(2)} \approx 130\hbar^2 \text{ MeV}^{-1}$  (an average over  $g^{(2)}$  from  $2g^{(2)} \approx 120\hbar^2 \text{ MeV}^{-1}$  to  $140\hbar^2 \text{ MeV}^{-1}$ , see Fig. 1).

(iii) On the basis of the estimated multiplicity and changes in the energy landscape with  $I$  we

suggest that the valley with  $2g^{(2)} \approx 176\hbar^2 \text{ MeV}^{-1}$  corresponds to a superdeformed configuration with  $\beta_2 \approx 0.06$  and spins around  $I = 54\hbar$ .

This work was supported in part by the Polish-American Maria Skłodowska Fund, Grant No. P-F7F037P.

<sup>(a)</sup>Permanent address: Institute of Physics, Technical University, Koszykowa 75, PL-00-662 Warsaw, Poland.

<sup>1</sup>J. C. Merdinger, F. A. Beck, T. Byrski, C. Gehring-er, J. P. Vivien, E. Bozek, and J. C. Styczen, Phys. Rev. Lett. **42**, 23 (1979); T. L. Khoo, R. K. Smither, B. Haas, O. Häusser, H. R. Andrews, D. Horn, and D. Ward, Phys. Rev. Lett. **41**, 1027 (1978).

<sup>2</sup>T. L. Khoo, J. Phys. (Paris), Colloq. **41**, C10-9 (1980).

<sup>3</sup>J. P. Vivien, Y. Schutz, F. A. Beck, T. Byrski, C. Gehring-er, and J. C. Merdinger, Phys. Lett. **85B**, 325 (1979).

<sup>4</sup>C. G. Andersson, S. E. Larsson, G. Leander, P. Möller, S. G. Nilsson, I. Ragnarsson, S. Åberg, R. Bengtsson, J. Dudek, B. Nerlo-Pomorska, K. Pomorski, and Z. Szymanski, Nucl. Phys. **A268**, 205 (1976).

<sup>5</sup>J. Dudek, T. Werner, C. Dasso, and T. Dössing, to be published; Warsaw-Tübingen collaboration, to be published.

<sup>6</sup>G. Leander, Y. S. Chen, and B. S. Nilsson, Phys. Scr. **24**, 164 (1981), and references therein.

<sup>7</sup>J. Dudek, A. Majhofer, W. Nazarewicz, and Z. Szymanski, to be published.

<sup>8</sup>O. Andersen, J. D. Garrett, G. B. Hagemann, B. Herskind, D. L. Hillis, and L. L. Riedinger, Phys. Rev. Lett. **43**, 687 (1979).

<sup>9</sup>A. Majhofer, W. Nazarewicz, and T. Werner, to be published.

<sup>10</sup>B. Herskind, J. Phys. (Paris), Colloq. **41**, C10-106 (1980).

<sup>11</sup>G. B. Hagemann, R. Broda, B. Herskind, M. Ishihara, S. Ogaza, and H. Ryde, Nucl. Phys. **A245**, 166 (1975).

<sup>12</sup>R. Baas, Phys. Rev. Lett. **39**, 265 (1977).